

EXIMIUS: A Measurement Framework for Explicit and Implicit Urban Traffic Sensing

Zhou Qin
Rutgers University
zq58@cs.rutgers.edu

Zhihan Fang
Rutgers University
zhihan.fang@cs.rutgers.edu

Yunhuai Liu
Peking University
yunhuai.liu@pku.edu.cn

Chang Tan
iFlytek
changtan2@iflytek.com

Wei Chang
iFlytek
weichang2@iflytek.com

Desheng Zhang
Rutgers University
desheng.zhang@cs.rutgers.edu

ABSTRACT

Urban traffic sensing has been investigated extensively by different real-time sensing approaches due to important applications such as navigation and emergency services. Basically, the existing traffic sensing approaches can be classified into two categories, i.e., explicit and implicit sensing. In this paper, we design a measurement framework called EXIMIUS for a large-scale data-driven study to investigate the strengths and weaknesses of these two sensing approaches by using two particular systems for traffic sensing as concrete examples, i.e., a vehicular system as a crowdsourcing-based explicit sensing and a cellular system as an infrastructure-based implicit sensing. In our investigation, we utilize TB-level data from two systems: (i) vehicle GPS data from 3 thousand private cars and 2 thousand commercial vehicles, (ii) cellular signaling data from 3 million cellphone users, from the Chinese city Hefei. Our study adopts a widely-used concept called crowdedness level to rigorously explore the impacts of various spatiotemporal contexts on real-time traffic conditions including population density, region functions, road categories, rush hours, etc. based on a wide range of context data. We quantify the strengths and weaknesses of these two sensing approaches in different scenarios then we explore the possibility of unifying these two sensing approaches for better performance. Our results provide a few valuable insights for urban sensing based on explicit and implicit data from transportation and telecommunication domains.

Permission to make digital or hard copies of all or part of this work for personal or classroom use is granted without fee provided that copies are not made or distributed for profit or commercial advantage and that copies bear this notice and the full citation on the first page. Copyrights for components of this work owned by others than the author(s) must be honored. Abstracting with credit is permitted. To copy otherwise, or republish, to post on servers or to redistribute to lists, requires prior specific permission and/or a fee. Request permissions from permissions@acm.org.
SenSys '18, November 4–7, 2018, Shenzhen, China
© 2018 Copyright held by the owner/author(s). Publication rights licensed to ACM.

ACM ISBN 978-1-4503-5952-8/18/11...\$15.00
<https://doi.org/10.1145/3274783.3274850>

CCS CONCEPTS

• **Networks** → **Network measurement; Sensor networks;**

KEYWORDS

Telecommunication, transportation, network, measurement

ACM Reference Format:

Zhou Qin, Zhihan Fang, Yunhuai Liu, Chang Tan, Wei Chang, and Desheng Zhang. 2018. EXIMIUS: A Measurement Framework for Explicit and Implicit Urban Traffic Sensing. In *SenSys '18: Conference on Embedded Networked Sensor Systems, November 4–7, 2018, Shenzhen, China*. ACM, New York, NY, USA, 14 pages. <https://doi.org/10.1145/3274783.3274850>

1 INTRODUCTION

The road Crowdedness Level (CL), as a simplified indicator of traffic speed, has very important applications in urban areas, e.g., navigation [5] [11] and emergency response [16]. In particular, Google Maps [13] and Gaode Maps [12] (i.e., a major online map service provider in China) use different colors to imply different CLs on maps, which reflect a travel delay considering roads speed limits and provide hints for choosing alternative routes to save time. Compared to speed, CL with a low granularity enables a simplified calculation, estimation, and prediction for traffic conditions with a higher sensing and computational efficiency [24] [46].

Due to its importance, CL, or traffic condition in general, has been studied extensively by different sensing systems and their data. For example, vehicular systems and their GPS data [1] [39], loop sensors and their log data [42], cellular networks and their signaling data [19][8][22][44], and even building sensing systems and their occupancy data [45]. In short, the existing CL sensing approaches can be basically classified into *Explicit Sensing* and *Implicit Sensing* based on their sensing natures. The explicit sensing systems have direct CL measurements, e.g., vehicular systems and their GPS data as well as loop sensors and their log data. In contrast, implicit sensing systems have indirect CL measurements, e.g., (i) cellular networks and their signaling data, with which CLs

are calculated based on changes of cellphone user's attached cell towers along with the associated time interval [19]; (ii) sensing systems for buildings and their occupancy data, with which CLs are calculated based on a learned correlation between building occupancy level and nearby traffic conditions [45].

Even with the above state-of-the-art sensing approaches, real-time urban-scale CL is still challenging to model because of the spatiotemporal coverage and accuracy of sensing systems. For the explicit sensing, its advantage is the accurate measurement, but its spatiotemporal coverage is low due to low penetration rates [33] [34] [31] [35], and further its deployment cost is high due to dedicated purposes [40] [14]. Based on our research results in the Chinese city Hefei, we find that a 6-thousand-vehicle network can only cover 28% of the road segments in this city with a one-hour time slot. In contrast, for implicit sensing [18] [19] [8], its advantage is high spatiotemporal coverage due to its high penetration rates [41], but its CL measurement accuracy is low because of indirect measurements [10]. Besides, implicit sensing usually makes use of existing datasets, which are dedicated to other purposes [26] [6]. For example, based on our results, we find that the data from cellular networks can only provide 61% accuracy on predicting travel time since their CL modeling is based on tower-level locations. To date, it is still unclear which sensing approaches and their data are better for urban-scale CL modeling under what contexts [29]. Given numerous sensing approaches for CL sensing or traffic modeling in general, we are reluctant to provide another sensing approach. Instead, we are interested in the evaluation of which kinds of sensing systems are better in what scenarios, and how can we explore their individual strengths to collectively address their individual weaknesses.

To achieve this goal, we design a measurement framework called EXIMIUS (meaning excellent in Latin) to validate EXPLICIT and IMPLICIT solutions for Urban Sensing. In EXIMIUS, we utilize CL as a concrete metric to quantify the advantages and disadvantages of both explicit and implicit sensing. Different from the existing work focusing on either explicit or implicit sensing, EXIMIUS features a comparative study and explores (i) in which contexts (including spatiotemporal and contextual factors) one approach is better than the other, and (ii) how we can combine the strengths of these two approaches to overcome their individual weaknesses. In particular, the contributions of this paper are as follows.

- To our knowledge, we conduct the first quantitative investigation on traffic condition (quantified by CL) sensing approaches from explicit and implicit perspectives by utilizing two large-scale real-world infrastructures to address the trade-offs of two approaches considering different sensing features. Our study is mainly based

on real-world data from 5 thousand vehicles (GPS data), 3 million cellphones (signaling data) and 7 million residents (census data). Such large-scale infrastructures and data enable us to perform a detailed comparative study on explicit and implicit traffic sensing.

- We design a context-aware measurement framework called EXIMIUS based on GPS data from a vehicular system as an example of explicit CL sensing, and signaling data from a cellular network as an example of implicit CL sensing. With these data, we provide some in-depth analytic results about their spatiotemporal coverage and accuracy. We further compare pros and cons of two state-of-the-art models based on the data in various settings to evaluate the impacts of population density, region functions, road types, and the rush hours on the performance of these two CL sensing.
- We implement EXIMIUS with one month of 893-GB vehicular GPS data and cellular signaling data from Chinese city Hefei, along with context data including population data and road network data. To validate the coverage and accuracy of two kinds of data and their resultant models, we utilize navigation data from one of the largest navigation and map service providers in China as the ground truth for evaluation. To our knowledge, this is the first time that such detailed datasets are utilized to implement an urban traffic sensing project.
- Our measurement results reveal the impacts of various contextual information on CL sensing, providing insights on the trade-offs between spatiotemporal coverage and accuracy for real-world traffic sensing. Based on our results, we provide a detailed discussion of insights for explicit and implicit urban sensing and important lessons learned. Besides, we discuss the generality of EXIMIUS by explaining its ability to include more data sources, such as bicycles, buses, CDR, etc.
- Based on characteristics of explicit and implicit sensing, we provide a solution to improve spatiotemporal coverage and accuracy of traffic sensing by integrating these two kinds of sensing based on data fusion.

The rest of the paper is organized as follows. Section 2 describes explicit and implicit sensing systems and their data. Section 3 introduces two state-of-the-art models for explicit and implicit sensing. Section 4 shows our measurement results under different contexts. Section 5 discusses insights and lessons learned from our comparative analysis. Section 6 provides related work, followed by conclusion in Section 7.

2 EXIMIUS: SENSING SYSTEMS & DATA

To compare implicit and explicit sensing approaches, our measurement study focuses on the Chinese city Hefei, i.e., the capital city of Anhui Province with a total area of 4,372 mi^2

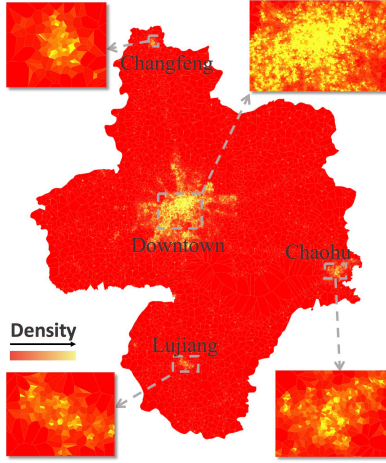


Fig 1: Voronoi Partition

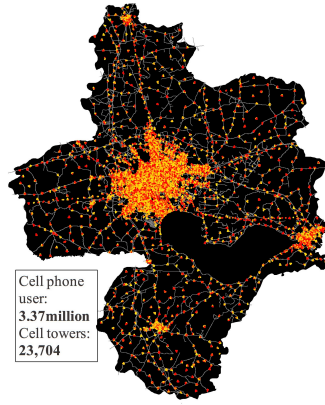


Fig 2: Roads and Cell Towers

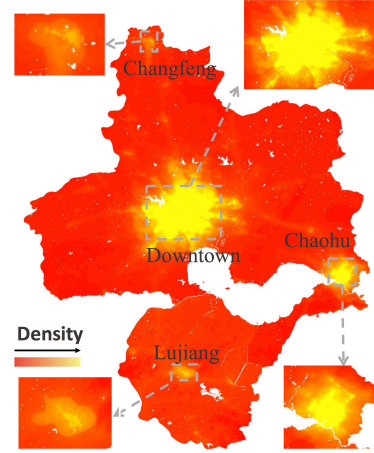


Fig 3: Population Distribution

and 7 million population. The two sensing systems we study in EXIMIUS represent two major urban sensing infrastructures from the telecommunication domain [18] [20] and the transportation domain [38] [25] [48] [21]. In Subsection 2.1 and 2.2, we present these two sensing systems and their sensing data. In Subsection 2.3, we introduce contextual data to understand their impact on sensing results. In Subsection 2.4, we describe how to quantify CLs under different spatiotemporal partitions.

2.1 Cellular System for Implicit Sensing

Based on our collaboration, we have offline data access to one of the three major cellular operators in China. This cellular network has 23,704 cell towers in Hefei and provides services for 3.37 million users with 20 GB records generated per day.

- **Timestamp:** Time when the record was generated at sub-second level.
- **Tower ID:** A unique identification of the cell tower from which the record was generated.
- **User ID:** A unique encrypted identification of the cell-phone user associated with this record.
- **Web Type:** The type of connection the user has established, e.g., 2G, 3G, 4G or LTE.
- **Service Type:** Seven service types in total, including Patch_Switch, CSFB (Circuit Switched FallBack), TAU (Tracking Area Update), LTE_ATTACH, LTE_DETACH, LTE_PAGING, Service_Req (e.g., 2G, 3G, 4G, LTE).

Spatial and Temporal Coverage: We first perform a detailed analysis of signaling data to validate their spatial and temporal coverage for CL modeling.

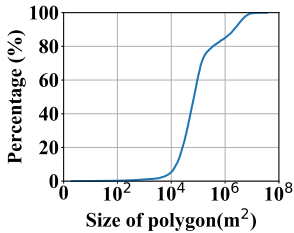


Fig 4: Cell Size Dist.

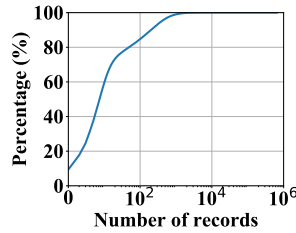


Fig 5: Record # Dist.

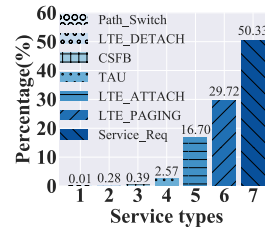


Fig 6: Record Type Dist.

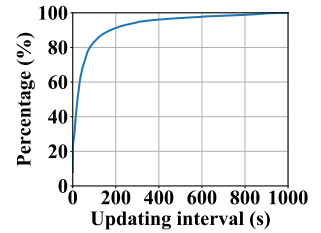


Fig 7: Updating Dist.

System Granularity: Based on all cell towers' locations, we obtain a Voronoi partition [2] of Hefei as in Figure 1. We find that this cellular network leads to a very detailed partition even on the cell tower level. A distribution of cell region sizes is given in Figure 4. We find that 85% of cell regions have a size smaller than 1 km² and 5% of regions in the downtown area have a size smaller than 0.01 km², making them fine-grained enough for crowdedness level sensing.

Data Format: Signaling data cover several events including cell tower attaching and detaching, etc. [19] The detailed format of signaling data is as follows.

As shown in Figure 5, we find that 60% users have more than 10 daily records, providing a large amount of data for urban sensing. For all the data generated, we find that more than 50% of signaling data are generated for Service Requests, e.g., phone call, SMS, Web services as shown in Figure 6, and a large number of them are for web services, e.g., social network apps, which require frequent data accessing. To further evaluate the data generating frequency, Figure 7 gives CDF of updating intervals, i.e., the time interval between two signaling records. We find that 80% of the records have an updating interval shorter than 100s and the average updating

interval is 70.26s, which indicate a large number of records can be used for CL modeling.

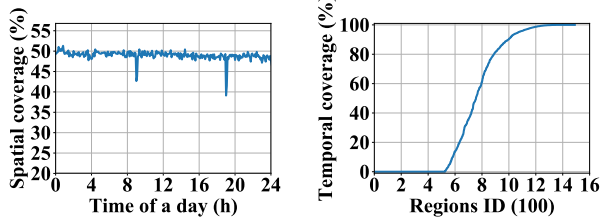


Fig 8: Cell Spatial Dist. Fig 9: Cell Temp. Dist.

In addition to the temporal aspect, we also analyze the spatial aspect of cellular network data for CL modeling on road segments. Based on location data of towers and roads, we visualize all 23,704 towers in Hefei and Hefei road network in Figure 2 to qualitatively show the spatial road network coverage of cell towers. Each dot represents one cell tower: a yellow dot indicates a higher amount of signaling data records generated in that tower and a red dot indicates a lower amount of that. We find that all major road segments' cell towers have a large number of data records, making CL modeling easier. We find that the cell towers are distributed densely in the downtown area and sparsely in the suburban and rural areas. There are 48.3% of road segments and 67.9% of towers covering the downtown area (around 6% of the Hefei area). We also find that almost all downtown road segments are associated with at least one tower.

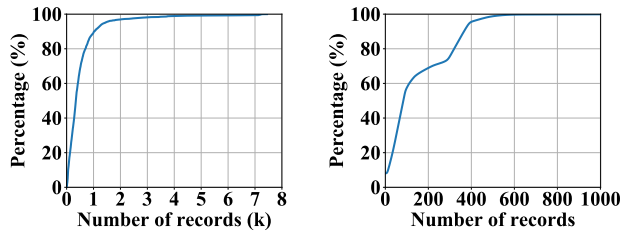


Fig 10: PV Uploading Fig 11: CV Uploading

To quantitatively investigate spatial and temporal coverage of the cellular network, Figures 8 and 9 give spatial and temporal coverage rates on the road segment level of 288 5-minute slots upon a day. We find that (i) 83% of road segments in downtown Hefei (48.7% of the entire Hefei) have at least one data record for every 5 minutes; (ii) almost all regions have at least one data record for every one of 288 slots. Such a detailed spatiotemporal coverage makes real-time CL sensing based on cellular network very complete.

2.2 Vehicular System for Explicit Sensing

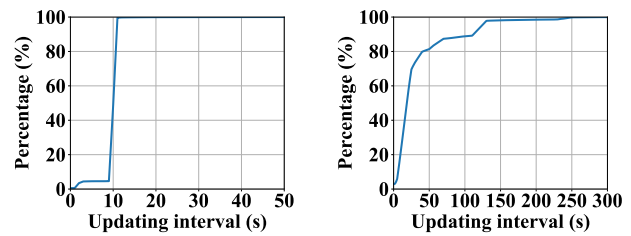
Based on our collaboration with a tech company, we have access to a vehicular network in Hefei with 2,887 private vehicles and 2,021 commercial vehicles, which are used to implement an explicit sensing approach for CL modeling.

Due to operating natures of these two kinds of vehicles, we study them separately as follows.

Data Format: With a GPS-level spatial granularity, both private and commercial vehicles are using on-board devices to generate data with the following format.

- **Timestamp:** Time when the record was generated at a level of seconds.
- **Vehicle ID:** A unique identification of a vehicle, from which the record was generated.
- **GPS Location:** A set of GPS coordinates indicate the location where the record was generated.
- **Speed:** A number from 0 to 200 indicating the speed of the vehicle when the record was generated.

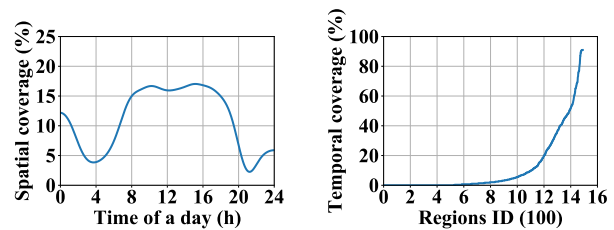
On average, all private and commercial vehicles upload 1.5 million and 500 thousand records to a central server per day with cellular connection based on their uploading frequency. In Figures 10 and 11, we find that 90% of private vehicles upload fewer than 1,000 records per day, whereas 80% of commercial vehicles upload fewer than 300 records per day.



(a) Private Vehicle Interval (b) Commercial Vehicle Interval
Fig 12: CDF of vehicular Updating Interval

In Figure 12, we further investigate the distribution of the updating intervals for these two kinds of vehicles. For the private vehicles, their average updating interval is around 10.17 seconds; whereas for the commercial vehicles, their average updating interval is around 33.88 seconds.

We qualitatively visualize the distribution of both private and commercial vehicle data on the road map in Figure 14 and 15 with their one-day data. We find that most of the road segments can be covered by either one of them. But a daily coverage is too coarse-grained for real-time CL modeling. To further evaluate their fine-grained spatial and temporal distributions, we show their coverage in 5 min slots in Figure 13.



(a) Spatial Coverage of GPS (b) Temporal Coverage of GPS
Fig 13: Spatiotemporal Coverage of Vehicular Systems

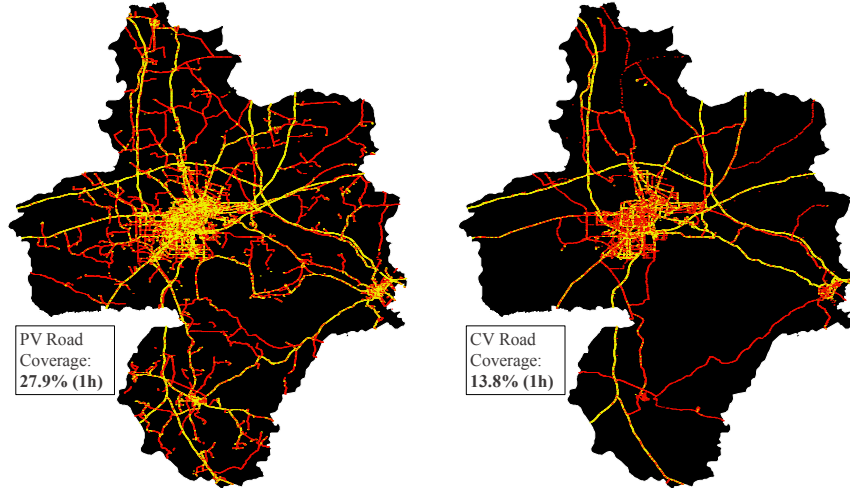


Fig 14: Private Vehicle Dist.

Fig 15: Commercial Vehicle Dist.

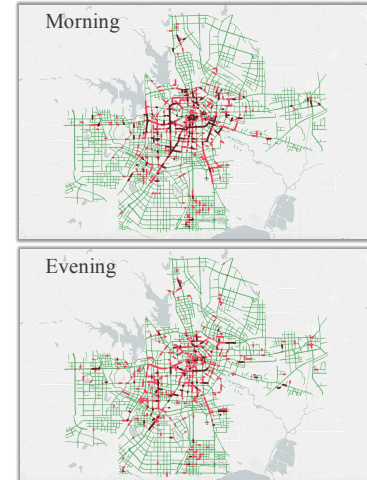


Fig 16: Ground Truth Data

We find that under such a fine-grained spatial and temporal granularity, coverage of explicit data is low, which makes it challenging for them to model CL in real time.

2.3 Contexts

To contextualize our CL modeling, we utilize two kinds of context data: (i) population, i.e., Worldpop data [32]; (ii) road networks, i.e., OpenStreetMap data [15].

Worldpop Data: Worldpop dataset is an open dataset [32], which provides static population with a spatial granularity of $100m \times 100m$ by fusing multiple data sources including survey data and satellite picture data. We visualize the population of Hefei in Figure 3. We find that most of the residents are living in the downtown area. Such a detailed dataset provides a valuable urban density context for us to understand the performance of implicit and explicit sensing approaches. The total population calculated by Worldpop data is 7.1 million, close to the population released by Hefei government.

Open Street Map Data: OpenStreetMap data [15] contain detailed roads and POI (i.e., points of interest) information in Hefei. In the OpenStreetMap data, each road segment is assigned with one of eight types, i.e., Motorway, Trunk, Primary, Secondary, Tertiary, Residential, Unclassified, and Service. Figure 17 gives the road types distribution in Hefei, and we find that 81.8 % of road segments are Motorway, Trunk, Primary, Secondary, Tertiary, and Residential, which can be covered by vehicular data we have. With the data from OpenStreetMap, we aim to understand the impact of different road types on the performance of two sensing systems.

2.4 Metrics: Crowdedness Level

In this paper, we utilize crowdedness level (CL) to quantify the final results from these two kinds of sensing approaches. The CL has been widely used in the online map services [13]

and transportation community [43] [27]. Formally, the CL is associated with a spatiotemporal combination, e.g., a 5-minute time slot and a road segment, and is quantified by a ratio of the extended travel time on this road segment for this particular time to the shortest travel time on this road segment during any time slot. Essentially, a bigger CL value indicates a longer travel time on the road segment.

Spatial Partition: In this paper, we study CL on two different levels: one is the road segment level where all road segments are given by Open Street Map; another is the Voronoi region level where all regions are given by a Voronoi graph. The road segment level CL works better for explicit vehicular sensing where we infer travel time on road segments and obtain CL directly; whereas the Voronoi level CL works better for implicit cellular sensing where we perform a more complicated inference process. We first find regions with at least one road segment within it (e.g., all Voronoi regions in the downtown have at least one road segment). For the region with multiple road segments, we then calculate a comprehensive CL by taking all road segments within this region into consideration and put weights on them according to the length of the road segment in this region. Compared to traditional spatial partition without logical contexts, such as straightforward grid partition, our context-aware partition enables a more balanced spatial units for CL modeling [36].

Temporal Partition: Considering the previous work [3] and the fact that 5-minute time slot is the finest temporal granularity we can have due to updating frequency of the ground truth data we introduce later, we evaluate different time slot lengths, i.e., 5, 10, and 20 minutes, in practical settings to test the performance of explicit sensing and implicit sensing on different temporal granularity. Further, to put our inference into high-level context, we also consider time of day as factor to evaluate their impacts on CL inference.

2.5 Ground Truth

For the evaluation purpose only, we have obtained datasets from one of the biggest navigation service companies in China. It provides real-time information about the crowdedness level of 47% of the road segments in the city, covering the entire downtown area of the city. Their real-time CL data are obtained by a proprietary solution based on data sources including traffic cameras, loop sensors, floating vehicles, etc. There are four different CL values ranging from 1 to 4, denoting an increasing traffic jam. Such detailed real-time CL data are very challenging to obtain at large-scale due to difficulty of extensive sensing infrastructures deployment[3]. We visualize all the road segments with the ground truth data in Figure 16 with four colors and we find that the ground truth data only cover the downtown area. During the evening rush hour from 8:00 to 9:00 pm, we have 89.0%, 8.7%, 1.5%, and 0.3% of road segments for four crowdedness levels, respectively. The lengths of different road segments are shown in Figure 18, from which we find that almost 95% road segments have a length of shorter than 0.5 km, enabling a fine-grained CL modeling.

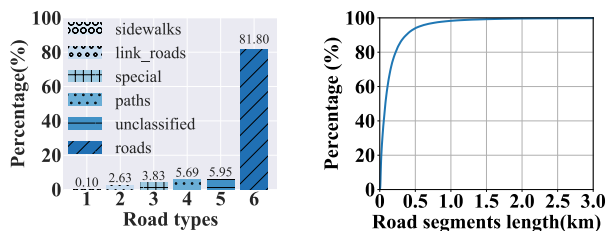


Fig 17: Road Type Dist.

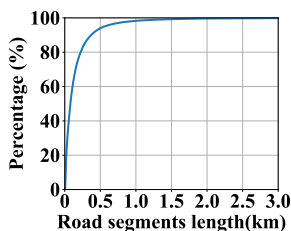


Fig 18: Segment Lengths

3 EXIMIUS: DATA-DRIVEN MODELS

Since our measurement framework EXIMIUS is aimed to evaluate two kinds of urban sensing approaches, instead of designing a new sensing model, we utilize the sensing systems and their data introduced in the last section to implement two state-of-the-art models.

3.1 Model Driven by Implicit Sensing Data

Among several state-of-the-art models for CL modeling (traffic condition modeling in general), we utilize the model from [19], which is the latest model using detailed cellular signaling data for travel time and crowdedness level inference. However, since this is a data-driven model, we utilize a few techniques to ensure our cellular signaling data can be used to implement this model.

Intuitively, the travel time can be extracted by simply considering two timestamps from two different cell towers. We show a test trace of a user with both GPS data and signaling data in Figure 19.

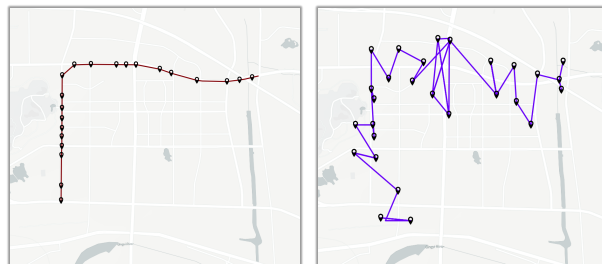


Fig 19: GPS and Signaling Trace of a User

The left figure visualizes the raw GPS data and the right figure presents the trace of attached cell towers. We find that two traces have high-level similarity, but the trace based on signaling data is more uncertain. In particular, consider the fact that the length of most road segments in Hefei road networks is shorter than 0.5 km (Figure 18), and the coverage radius of a cell tower is roughly 300 meters, it is challenging for us to estimate travel time on the road segment level. This is because the coverage distance can be as long as 600 meters, which is even greater than the length of road segments. This leads to large estimation error considering that a cellphone user standing on the border of two cell towers can be attached to either tower at any time due to the congestion control of the cellular networks, leading to a phenomenon called “Ping-Pong Effect” [17], meaning a cellphone user quickly moves between two cell towers.

In order to better validate claims above, we analyze some statistic features from the traces of GPS and signaling data of this one user and present the results in Table 1. The Ref. speed is a reference average speed calculated by real physical trace distance (5.9km) and absolute travel time (691s).

Table 1: Comparison of CL Estimation

Data	Ave. speed	Speed var.	Travel time	Ref. speed
GPS	10.0(m/s)	33.6	669.0(s)	8.84(m/s)
Signaling	100.1(m/s)	18671.51	690.0(s)	8.84(m/s)

We find that the speed calculation based on signaling data cause larger error compared to GPS data, but travel time is relatively accurate. Besides, it is not reasonable to calculate travel time between short distances, especially for a distance shorter than the coverage radius of one tower, since it will be challenging either to distinguish the moving status of a cellphone user or to estimate the travel time precisely. Thus, we choose relative longer real-world road segments as our target roads and implement the algorithm in [19] with extra constraints.

Based on Algorithm 1, we extract users who were actually traveling on vehicles by setting travel time and travel distance limits, then we can have all the cell pairs candidates in two driving directions. Actually, we find that setting limits for the distance of cell tower pairs is enough for outliers filtering. For a specific user, there may be multiple records, so we implement an intuitive algorithm for the final travel

Algorithm 1 Algorithm of selecting cell tower pairs

```

 $t_{max} \leftarrow$  maximum travel time of target road segment
 $t_{min} \leftarrow$  minimum travel time of target road segment
 $dist_{max} \leftarrow$  maximum distance of two cell towers
 $dist_{min} \leftarrow$  minimum distance of two cell towers
 $T \leftarrow$  set of cell towers in proximity of target road
for  $tower_i$  in  $T$  do
  for  $tower_j$  in  $T$  do
    if  $i \neq j$  and  $dis_{min} \leq distance(tower_i, tower_j) \leq dis_{max}$  then
      Calculate direction of cell tower pairs
      Calculate travel time of cell tower pairs
    end if
  end for
end for
Return cell tower pairs satisfying all conditions

```

time calculation [19]. The main idea is to consider (i) the last signaling record attached to the departure cell tower, (ii) the first signaling record attached to the arrival cell tower, and (iii) the average travel time for different users.

We utilize a highway segment given in Figure 20 called national highway G206 to show an example of how to calculate the travel time based on signaling data [19]. This segment of national highway G206 has a total length of 8.2 km and the maximum speed for the road is 120 km/h (i.e., corresponding to a travel time of 4.2 minutes). There are 235 towers in proximity and 1,618 different road segments on this road, and 9,153 users during a day recorded by signaling log. The maximum number of records for a single user is 2,252; the minimum number is 2; the average number is 40. Based on the travel time calculation algorithm, we then convert the resultant travel time into the CL by speed ranges of four CLs.

3.2 Model Driven by Explicit Sensing Data

Based on explicit sensing data, we implement a travel time estimation model to obtain CLs for all road segments with different time intervals. Given the historical GPS data we have and features of these data, we implement the model from [3] as our explicit sensing model, where an algorithm focusing on creating a prediction table by referring to historical GPS data at the same region partitioned and similar time is introduced. Even though some models are proposed recently [42], they either require additional datasets or their model descriptions are at a high level, and cannot be implemented with details for a fair comparison.

During the implementation of our explicit sensing model, we utilize a spatial partition based on Voronoi polygons generated by locations of cell towers in order to provide a fair comparison with signaling data. As for the temporal

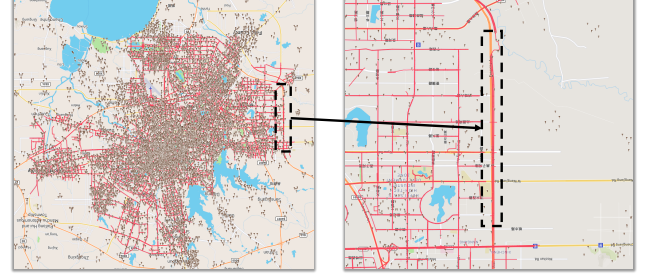


Fig 20: Example of Highway Segment

aspect, we still consider the similar partition, i.e., time of the day. Inputs of the model are raw GPS data from private vehicles and commercial vehicles. They are formatted into traces by different users and different time periods. Different from storing historical travel durations into entries, we store crowdedness level into entries for two reasons: i) we directly compare CL derived from signaling data in the end, so it would be more efficient for us to store CL directly; ii) it is challenging to calculate travel durations given specific boundaries of polygon regions since the segmentation of trips is needed. However, after converting travel time to CL, we can easily obtain CL status by examining how the CL calculated by this trip contributes to the actual overall CL of the corresponding roads.

Algorithm 2 Algorithm of travel time prediction

```

 $T \leftarrow$  All traces of users
 $P \leftarrow$  All Voronoi polygons
 $M \leftarrow$  Matrix storing historical CL data
 $m_{pt} \leftarrow$  CL of time period  $t$  and polygon region  $p$ 
for  $trace$  in  $T$  do
  Convert travel time to CL
  if  $m_{pt}$  does not exist then
    Create an entry under this context
    Assign value of CL to the entry
  else  $m_{pt}$  exists
    Append value of current CL to  $m_{pt}$ 
  end if
end for
Update  $M$  with weighted entries
return  $M$ 

```

Note that we do not average all the historical data directly, instead we consider the values of different CL within specific time and location to improve the accuracy in our case. The detailed are given in Algorithm 2 [3].

4 MEASUREMENT RESULTS

In this section, we show our measurement results from CL modeling. In order to comprehensively compare these two

kinds of sensing approaches, we consider several factors affecting the performance of traffic sensing, i.e., evaluation sites (Subsection 4.1), spatial impacts (Subsection 4.2), temporal impacts (Subsection 4.3), and contextual information (Subsection 4.4).

4.1 Comparisons on Four Evaluation Sites

Since different road types typically have different speed limits and traffic volume capacities, we perform a data-driven investigation of four kinds of road types based on Hefei road networks. We report our results in detail based on four roads from four kinds of these road types. These four roads have different road lengths from 0.9 km to 2.6 km, and have different number of road segments from 395 to 2,782, and are from different urban regions around the city, i.e., commercial area, residential area, industrial area, and airport highway area. By considering all these possible features regarding road segments we can make sure our evaluation sites are representative. The average statistical characteristics from these four roads are given in Table 2.

Table 2: Statistics of Road Segments

Context	Road 1	Road 2	Road 3	Road 4
Road type	avenue	main ave.	motorway	highway
Road len.(km)	2.23	1.9	0.9	2.6
# of segment	1595	395	1709	2782
# of GPS users	273	509	680	710
# of GPS recs	14,921	11,342	65,314	81,100
# of towers	403	365	804	1017
# of tele users	76,615	92,976	240,549	246,324
# of tele recs	3,504,747	4,126,435	10,429,728	10,723,447

To compare cellphone-based explicit sensing and vehicle-based implicit sensing, we combine private vehicles GPS data and commercial vehicles GPS data together as vehicular data to implement the explicit CL sensing model described in Section 3.2. We compare this model with the implicit CL sensing model based on the telecommunication data, i.e., signaling data, described in Section 3.1. From the table above, we find that in our dataset, the implicit sensing data, i.e., signaling data, have much more records and users logged during a day compared to the explicit sensing data, i.e., vehicle GPS data. One reason is that we have much more cellphone users than car users; another reason is that signaling data update much more frequently, leading to a higher temporal coverage rate. With these data, we calculate the results of the CL inference of these four sample roads and then compare them with the ground truth data introduced in Section 2.5. The detailed results are summarized in Table 3.

From the above results, we find that with a 5-minute slot length setting, the temporal coverage rate of vehicle-based explicit sensing is lower than that of cellphone-based implicit sensing across all evaluation roads. Even though their

Table 3: Comparison of CL Estimation

Context	Road 1	Road 2	Road 3	Road 4
Accuracy (Explicit) (%)	98.6	97.2	98.6	98.6
Coverage (Explicit) (%)	44.4	45.8	45.8	86.1
Accuracy (Implicit) (%)	61.1	73.6	62.5	73.6
Coverage (Implicit) (%)	100	100	100	100
Explicit CL var.	0.52	0.31	0.26	0.08
Implicit CL var.	0.22	0.03	0.04	0.16
Ground Truth CL var.	0.17	0.18	0.22	0.05

overall temporal coverage rates are smaller than these of implicit sensing data, explicit sensing data enable a sensing approach with better accuracy, which verifies our previous observation that cellphone-based implicit sensing has better coverage, but vehicle-based explicit sensing has higher accuracy. Further, by calculating the CL variance, we find that a smaller variance normally corresponds to a higher estimation accuracy in both cellphone-based implicit sensing and vehicle-based explicit sensing for the CL estimation.

4.2 Spatial Factors

Traffic sensing is also heavily affected by following spatial factors: (i) urban region functions, e.g., the downtown area may be more crowded, and a rural area may be less crowded; (ii) road lengths, e.g., the longer road may have more vehicles and more cellphone users to contribute data; (iii) road types, e.g., the highway may have less traffic jam compared to other road types. Thus, we further explore impacts of spatial contextual information on two sensing approaches.

Based on Figure 21, the CL prediction results from both sensing approaches indicate that highway has a higher prediction accuracy than other road types, e.g., Road 4 has the best performance. Further, the road length may have a big impact on the prediction results since the shortest Road 3 has the biggest Mean Absolute Percentage Error (MAPE) value compared to other roads. For all results, it seems that the MAPE value is inversely proportional to road lengths, indicating that the CL prediction on a shorter road segment may cause larger errors. This is because there are fewer data points when the road is shorter, sparse data points may bring biases since they cannot accurately reflect the real traffic status of road segments. Finally, the cellphone-based implicit sensing has a lower CL prediction accuracy in general compared to vehicle-based explicit sensing except for the highway, which contains enough signaling data across cell towers to estimate CLs.

In addition to road-based setting, we also implement a region-based CL prediction for these two approaches based on Voronoi regions. For cellphone-based implicit sensing, we calculate user density and population density from Worldpop data, also consider CLs inferred by users' switching between different towers, and then implement prediction by a regression model. For vehicle-based explicit sensing, we implement

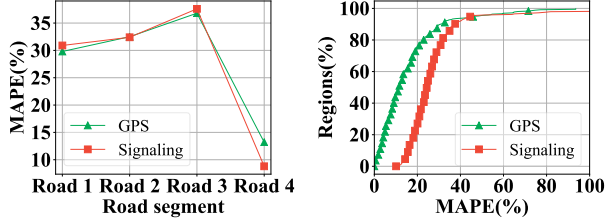


Fig 21: Road Accuracy Fig 22: Region Accuracy

a state-of-the-art model [3] by first partitioning the whole city in 5 thousand grids and then locating Voronoi regions in these grids, saving time to locate the entries of each GPS point for the later prediction. Once we obtain a user's location, we first locate it in large grid partitions, and then locate its associated Voronoi polygon. Finally, we store each user's speed and timestamp as an entry into matrix. Results from two data sources are shown in Figure 22 based on a 5-minute time slot temporal partition. Based on the results, we find that for region-based CL sensing, vehicle-based explicit sensing still outperforms cellphone-based implicit sensing, which is consistent with our previous observation.

4.3 Temporal Factors

Different time of day can directly affect traffic status, e.g., traffic will be more crowded during rush hours. Since the CLs of the rush hours are more important due to the potential higher traffic demand, we study the temporal contexts during six hours, i.e., 6-7, 7-8, and 8-9 in the morning representing the morning rush hours; 16-17, 17-18, and 18-19 in the afternoon representing the evening rush hours. The time slot length, as another temporal factor, is also vital to our traffic sensing performance. We use 5, 10, and 20 minutes time slots to test their performance on different temporal granularity. In all, we show the CL prediction performance at both different time of day, and in different time slots.

Based on our previous Voronoi region partition, we investigate the traffic CL prediction based on Voronoi regions by randomly selecting 1,000 regions in Hefei downtown area where Ground Truth data are available with their specific features on the Voronoi polygon size, the number of cellphone users, and the number of population from Worldpop data. In particular, we divide a one-month CL dataset into 29-day training data and 1-day testing data, and after rotating the test data among 30 days, the average results were reported.

In Figure 23, we show estimation MAPE of the 1,000 regions from downtown area during morning and evening rush hours in 5-minute slots, based on historical CL data. We find that the MAPE values are similar in these six rush hours. Further, 08h00 and 18h00 have higher MAPE compared to other four rush hours, respectively. These results match the trend of CL during a day in Figure 24 (where 1 means no traffic jam and 4 denotes heavy traffic jam), showing that

these two hours are the most crowded time period in one day. We calculate the variance of Ground Truth CL of 6 hours on the same regions, and we find that these two hours have relatively higher variance than other four hours. As a result, a lower fluctuation may provide a better estimation of the CLs due to better sensing.

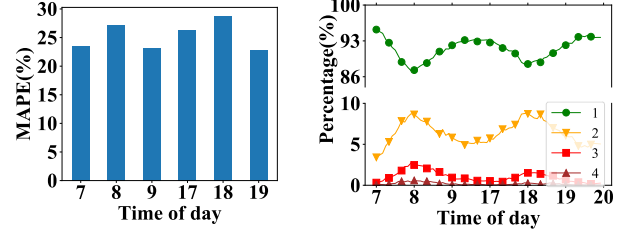


Fig 23: CL Prediction Fig 24: Gaode CL Dist.

For cellphone-based implicit sensing, we show the impact of different time slot lengths on the CL prediction results in Figure 25. We find that as we increase the length of the time slot from 5 to 20 minutes, MAPE generally decreases. This is because the CL in a longer time slot, e.g., 20 minutes, is easier to predict due to less fluctuation and more data collected compared to the CL in a shorter time slot, e.g., 5 minutes. Further, we explore the CL prediction results during different time of day in Figure 26. In particular, we average the accuracy within an hour based on different time slot lengths. We find that generally 8h00 and 18h00 have higher prediction error. This is because these two hours are with highly dynamic traffic demand across the city and even the ground truth varies significantly during short time periods, which lead to higher prediction errors.

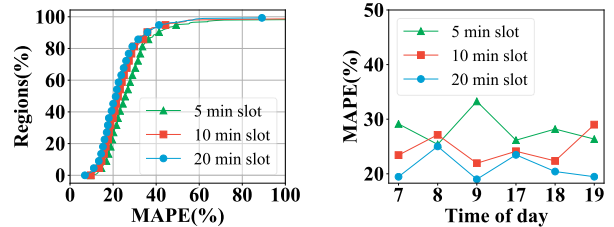


Fig 25: Temp. of Phone Fig 26: 6 Hour of Phone

For vehicle-based explicit sensing, we show the impact of different time slot lengths on the CL prediction results in Figure 27 and the impact of time of day on CL prediction results in Figure 28. We find some similar trends as results from cellphone-based implicit sensing. In particular, a relative long time slot leads to a smaller MAPE value, i.e., higher CL prediction accuracy. Similarly, 8h00 and 18h00 have relatively lower prediction accuracy, matching the results from cellphone-based implicit sensing due to high traffic demand.

Finally, we compare results of vehicle-based explicit sensing and cellphone-based implicit sensing. We find that as

shown by Figure 25 and Figure 27, given the same temporal granularity, i.e., the same time slot length, vehicle-based explicit sensing has a lower MAPE (i.e., higher accuracy). Similarly, as shown by Figure 26 and Figure 28, we find for the same time of day, vehicle-based explicit sensing has a lower MAPE compared to cellphone-based implicit sensing. The above results indicate that given the same time of day and the same time slot length, vehicle-based explicit sensing has better performance in terms of CL prediction than cellphone-based implicit sensing.

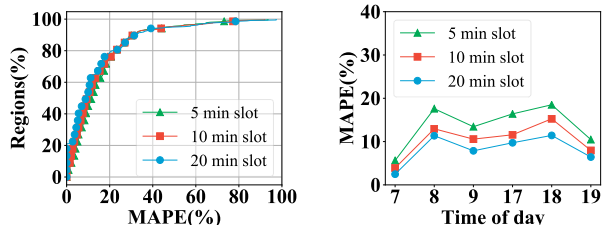


Fig 27: Temp. of Vehicle Fig 28: 6 Hour of Vehicle

Besides, we also show estimation results from non-rush hours upon our four sample roads by implicit sensing (Figure 29) and explicit sensing (Figure 30), compared to the Ground Truth data from the navigation service provider. We find that generally, explicit sensing has better performance than implicit sensing and Road 4 (highway) has a smaller estimation error. One possible explanation is that for the non-rush hour, the implicit sensing is only based on limited cellphone data, which leads to poorer performance.

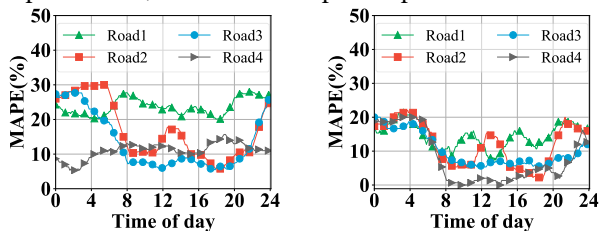


Fig 29: Temp. of Implicit Fig 30: Temp. of Explicit

4.4 Contextual Factors

Traffic sensing may also be influenced by other contextual factors, such as region size, population density, and user density, e.g., more users may indicate a higher traffic volume. We show how the contextual information influences the final inference result, aiming to provide insights into how to improve CL inference accuracy. Based on the Voronoi regions, we present our prediction results from ascending sorted polygon sizes, population density, and user density. The results are in Figures 31, 32 and 33, respectively. It is shown in Figure 31 that MAPE decreases as regions' sizes increase, which indicates larger regions can have better CL prediction accuracy, it is because larger regions include more

road segments. We find that the MAPE increases (i.e., CL prediction accuracy decreases) if there are a higher population or more users in the polygon, indicated by Figure 32 and 33.

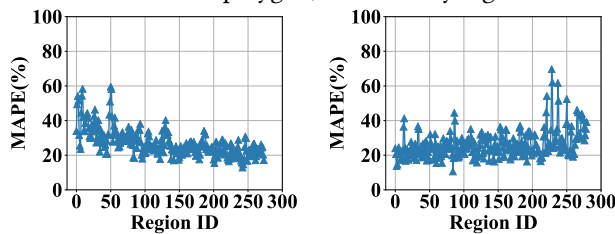


Fig 31: Polygon Size

Fig 32: Population

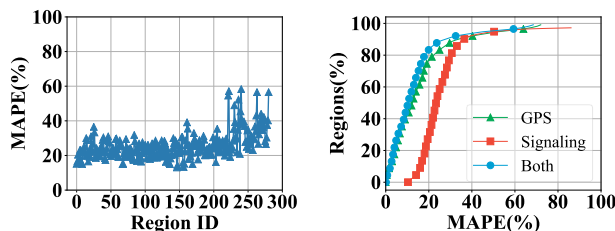


Fig 33: User Number

Fig 34: Integration

4.5 Integration of Two Sensing Approaches

Based on these two sensing approaches, we discuss the possibility of integrating two sensing approaches by one general model. Considering that we can infer CL by either cellphone-based implicit sensing or vehicle-based explicit sensing, we then have two different time series of CL. In this case, two CL series are complementary to each other if one (i.e., vehicle-based explicit sensing) lacks enough coverage rates under a specific temporal period and the other (i.e., cellphone-based implicit sensing) lacks accurate measurements.

Intuitively, fusing two time series can have a better spatiotemporal coverage than themselves alone. Further, more travel time records within certain regions can essentially reveal more information regarding actual traffic condition. In particular, we convert speeds to CLs according to a standard provided by the navigation service provider, which considers both road segments types and corresponding speed limits. We then have two series of CL data from signaling and GPS. For each time slot, if there is only one value from two series, we use this value; if there are two values, we take average of the two values. By this fusion we have better spatiotemporal coverage, estimation and prediction accuracy.

We show an example here by taking consideration of both signaling data and GPS data as traces of users to estimate and predict CL in four roads we mentioned above. The results are shown in the following Table 4. The estimation part here is to directly calculate CLs by both cellphone-based implicit sensing and vehicle-based explicit sensing. For the signaling data, we consider traces of moving users and their average

Table 4: Comparison of CL Estimation and Prediction

MAPE		Road 1	Road 2	Road 3	Road 4
Estimate	GPS (%)	56.3	57.6	42.3	11.1
	Signaling (%)	31.9	14.6	20.8	23.6
	Fusion (%)	23.6	17.4	18.1	9.7
Predict	GPS (%)	29.5	32.1	37.5	7.1
	Signaling (%)	30.3	32.1	37.9	11.5
	Fusion (%)	28.2	32.4	37.2	6.9

travel time; for the GPS data, we obtain users' speeds and convert it into CLs. We find that, generally, MAPE values decrease by using two datasets for an integrated sensing approach. We also fuse two data sources on the Voronoi region level. In particular, based on a specific data source (e.g., the cellphone signaling data), we integrate calculated CLs from different road segments on the same Voronoi region based on the method introduced in Section 2.4. For each region, we calculate a comprehensive CL by considering all road segments within this region and put weights on them based on the road segment length in this region. We then perform the similar process based on the other data source (e.g., the vehicular GPS data), and finally we use the average CL from these two methods as our final CL result in this particular region. The results are given in Figure 34. We find that by combining two datasets as an integrated sensing approach, it outperforms both individual sensing approaches based on GPS or signaling data alone. We expect a more sophisticated fusion approach which will further improve the results by considering the weights on different data sources instead of a straightforward averaging approach, which is out of the scope of this work and will be considered in our future work due to space limitation.

5 DISCUSSIONS AND LESSONS LEARNED

In this section, we discuss a few insights we obtained in our measurement study and some lessons learned.

Limitations: In this work, we only use data from a particular city Hefei for a measurement study for explicit and implicit sensing, so the results and conclusions obtained in this work may only apply to Hefei and cities with similar features, such as spatiotemporal coverage of data, updating frequency of data, population distribution, etc. We believe if the key factors such as statistic features of vehicular and cellular data, and contextual information are similar among cities, our results then can be generalized because they are the basis of all the above analyses. Further, we study the traffic conditions based on pre-defined spatial partitions, which may not be the optimal partition for traffic condition modeling. However, in general, how to partition cities into different regions to understand traffic condition or human mobility is still an open question [3].

Spatial Coverage: As shown in Figures 8 and 13, cellular and vehicular networks have different spatial coverages. In

general, cellular networks as an example of implicit sensing have better spatial coverage than vehicular networks as an example of explicit sensing. However, the spatial coverage of cellular networks is fixed because of the stationary natures of cell towers. In contrast, the spatial coverage of vehicular networks is dynamic due to mobile natures of vehicles. This indicates cellular networks can cover more regions, but vehicular networks are more flexible.

Temporal Coverage: As shown in Figures 9 and 13, we find that for cellular networks as implicit sensing, their temporal coverage is very high for some regions, indicating cellular networks always have data for these regions. However, for some remote regions, if there is no cell tower deployed in these regions, their temporal coverage is always 0. In contrast, for vehicular networks as explicit sensing, they have covered almost all regions, but the distribution is non-uniform, e.g., lots of regions with 20 slots covered among 288 slots, making it less ideal for continuous modeling.

Performance Comparison: We find that the prediction results for crowdedness levels by explicit sensing and implicit sensing approaches have their own advantages and disadvantages, in terms of coverage and accuracy. Which approach to use should be based on a set of factors related to system availability, cost, granularity, etc. Our study reveals some advantages of either explicit or implicit sensing in some concrete settings, and the details can be found among measurement results.

Data Collection: All the data used in this project are legally collected by the service providers. The data from commercial vehicles are collected by a logistic company who owns and manages these vehicles. The private vehicle data are collected by a large insurance company by an onboard device and smartphone app, and all customers are informed about data collection and agreed to provide their data for the company and its business partners for business analyses. In return, they received monthly premium reductions. Finally, all the cellular signaling data are also collected under the consent of the cellphone users by signing the contracts.

More Implicit and Explicit Sensing: Due to limited data access, we only consider a cellular network as an example of implicit sensing and a vehicular network as an example of explicit sensing. However, our framework can also be generalized by other real-world datasets, which can be treated as explicit and implicit sensing data. We aim to further explore other urban systems to improve our analysis, if the system users opt to participate under privacy preserving mechanisms, e.g., (i) image data from the traffic cameras or the cameras inside the transit systems as implicit sensing, (ii) data of a growing bicycle network with 8,000 bicycles in Hefei for rentals using the smart cards as implicit sensing, (iii) CDR data and cellular traffic data collected from telecommunication systems.

Privacy: While understanding traffic condition is beneficial for city residents, we have to protect the privacy of involved residents, i.e., cellphone users and vehicle drivers. In this project, all data analyzed are anonymized by the data provider and the analyzed data cannot be used to trace back to individual cellphone users or private and commercial drivers; we only process data related to traffic condition modeling and delete other non-relevant information to reduce risk; finally, in this work, all our analysis results on traffic conditions are given at aggregated cell tower or road segment levels instead of location for a specific timestamp, thus they cannot be used to trace back to individuals.

6 STATE OF THE ART

In general, there are many approaches in estimating and predicting real-time traffic conditions based on different sensing systems and their data. In this paper, we divide them into two categories, i.e., explicit sensing and implicit sensing.

Explicit Sensing: To explicitly sense the traffic conditions, many systems have been proposed. There are online map services, e.g., Google Map[13] and Gaode Map[12], which are mostly based on crowd-sourcing and smartphone apps. They utilize their users' GPS locations and speeds to model and predict traffic speeds with good accuracy. Another major direction is about onboard GPS devices in both private cars and commercial vehicles such as taxis [3], buses [47] and trucks [4][30]. In particular, Aslam et al. [1] present a system to use taxis as roving sensors to infer city-scale traffic conditions. Besides, traffic infrastructures (such as loop sensors and traffic cameras) are the most direct methods for traffic volume and traffic speed modeling [9]. For example, researchers propose various models for traffic estimation based on the image data obtained by traffic cameras and achieved high accuracy [7][23]. However, as we show in our measurement results, these solutions have the problems with low penetration rates and uncertain mobility patterns of sensing devices, e.g., vehicles and smartphone users.

Implicit Sensing: The key rationale for implicit sensing is low-cost data collection and high spatiotemporal coverage. For example, the telecommunication infrastructure has been utilized to infer traffic conditions given that there are already massive datasets collected from telecommunication systems, e.g., Call Detail Record (CDR) [37], WiFi data [34], signaling data [18][19][8], etc. These datasets reveal coarse-grained locations and time associated with these locations, which can be used to infer traffic conditions. Moreover, these infrastructure data are almost free, since they are automatically collected by existing infrastructures [10]. Considering the ubiquity of cellphones, cellular data thus have extremely high spatiotemporal rates. There are data records as long as there are people with cellphones and they even do not have

to use their cellphones. For example, the first set of work utilizing cellular data [28] to estimate the traffic conditions is based on the idea of utilizing mobile phones as traffic probes because this infrastructure is already in place in most urban areas, e.g., traffic speed information can be obtained by passively monitoring data transmission in the cellular network. Further, Janecek et al. [18] [19] utilize signaling data from both active and inactive cellphone users to infer traffic jam and achieved gain in coverage and accuracy by performing two-stage estimation on signaling data.

Summary: As we have shown in our work, both of these two approaches have strengths and weaknesses, and we need to carefully examine features of a particular city and sensing infrastructures for the best results of traffic modeling in a real-world setting.

7 CONCLUSION

In this paper, by designing and implementing EXIMIUS, we utilize two large-scale urban systems and traffic crowdedness level as examples to quantify, measure, and understand both explicit and implicit urban sensing approaches. Our EXIMIUS is based on a 3-million-user cellphone network and a 6-thousand-vehicle network along with their 1TB log data and various context data to provide a few novel insights on explicit and implicit urban sensing. Based on our measurements and comparative results in Hefei, we share a few lessons learned, which we believe will help fellow researchers when choosing from explicit and implicit urban sensing approaches. First, neither explicit vehicle-based sensing nor implicit cellphone-based sensing can provide both high spatiotemporal coverage and high accuracy for traffic crowdedness level modeling. The explicit vehicle-based sensing has better accuracy whereas the implicit cellphone-based sensing has higher spatiotemporal coverage. Second, various urban context information, e.g., population, road types, the rush hours, functions of regions, can provide additional accuracy and coverage, but their impacts on explicit vehicle-based sensing and implicit cellphone-based sensing are quite different. Last but not least, we show that a straightforward hybrid approach by combining explicit vehicle-based sensing and implicit cellphone-based sensing only on data level can provide significant improvement for both spatiotemporal coverage and accuracy.

ACKNOWLEDGMENTS

This work is partially supported by Rutgers Global Center, Rutgers Research Council, China 973 Program (2015CB352400), National Natural Science Foundation of China (NSFC) 41401470, 61772026 and 61332018, and National Key R&D Program of China 2018YFB0803400.

REFERENCES

- [1] ASLAM, J., LIM, S., PAN, X., AND RUS, D. City-scale traffic estimation from a roving sensor network. In *Proceedings of the 10th ACM Conference on Embedded Network Sensor Systems* (2012), ACM, pp. 141–154.
- [2] AURENHAMMER, F. Voronoi diagrams—a survey of a fundamental geometric data structure. *ACM Computing Surveys (CSUR)* 23, 3 (1991), 345–405.
- [3] BALAN, R. K., NGUYEN, K. X., AND JIANG, L. Real-time trip information service for a large taxi fleet. In *Proceedings of the 9th international conference on Mobile systems, applications, and services* (2011), ACM, pp. 99–112.
- [4] CASTRO, P. S., ZHANG, D., AND LI, S. Urban traffic modelling and prediction using large scale taxi gps traces. In *International Conference on Pervasive Computing* (2012), Springer, pp. 57–72.
- [5] CHEN, C. P., ZHOU, J., AND ZHAO, W. A real-time vehicle navigation algorithm in sensor network environments. *IEEE Transactions on Intelligent Transportation Systems* 13, 4 (2012), 1657–1666.
- [6] CHENG, Y., CHEN, K., ZHANG, B., LIANG, C.-J. M., JIANG, X., AND ZHAO, F. Accurate real-time occupant energy-footprinting in commercial buildings. In *Proceedings of the Fourth ACM Workshop on Embedded Sensing Systems for Energy-Efficiency in Buildings* (2012), ACM, pp. 115–122.
- [7] CUCCHIARA, R., PICCARDI, M., AND MELLO, P. Image analysis and rule-based reasoning for a traffic monitoring system. *IEEE Transactions on Intelligent Transportation Systems* 1, 2 (2000), 119–130.
- [8] DERRMANN, T., FRANK, R., VITI, F., AND ENGEL, T. Estimating urban road traffic states using mobile network signaling data. In *Abstract book of the 20th International Conference on Intelligent Transportation Systems* (2017).
- [9] DU, R., CHEN, C., YANG, B., LU, N., GUAN, X., AND SHEN, X. Effective urban traffic monitoring by vehicular sensor networks. *IEEE Transactions on Vehicular Technology* 64, 1 (2015), 273–286.
- [10] FU, M., KELLY, J. A., AND CLINCH, J. P. Estimating annual average daily traffic and transport emissions for a national road network: A bottom-up methodology for both nationally-aggregated and spatially-disaggregated results. *Journal of Transport Geography* 58 (2017), 186–195.
- [11] GAO, Y., SWAMINATHAN, K., CUI, Z., AND SU, L. Predictive traffic assignment: A new method and system for optimal balancing of road traffic. In *Intelligent Transportation Systems (ITSC), 2015 IEEE 18th International Conference on* (2015), IEEE, pp. 400–407.
- [12] GAODE. Gaode map. <https://ditu.amap.com>, 2017.
- [13] GOOGLE. Google map. <https://www.google.com/maps>, 2017.
- [14] HABIBZADEH, H., QIN, Z., SOYATA, T., AND KANTARCI, B. Large-scale distributed dedicated-and non-dedicated smart city sensing systems. *IEEE Sensors Journal* 17, 23 (2017), 7649–7658.
- [15] HAKLAY, M., AND WEBER, P. Openstreetmap: User-generated street maps. *IEEE Pervasive Computing* 7, 4 (2008), 12–18.
- [16] INOUE, Y., SASHIMA, A., IKEDA, T., AND KURUMATANI, K. Indoor emergency evacuation service on autonomous navigation system using mobile phone. In *Universal Communication, 2008. ISUC'08. Second International Symposium on* (2008), IEEE, pp. 79–85.
- [17] INZERILLI, T., VEGNI, A. M., NERI, A., AND CUSANI, R. A location-based vertical handover algorithm for limitation of the ping-pong effect. In *Networking and Communications, 2008. WIMOB'08. IEEE International Conference on Wireless and Mobile Computing*, (2008), IEEE, pp. 385–389.
- [18] JANECEK, A., HUMMEL, K. A., VALERIO, D., RICCIATO, F., AND HLAVACS, H. Cellular data meet vehicular traffic theory: location area updates and cell transitions for travel time estimation. In *Proceedings of the 2012 ACM Conference on Ubiquitous Computing* (2012), ACM, pp. 361–370.
- [19] JANECEK, A., VALERIO, D., HUMMEL, K. A., RICCIATO, F., AND HLAVACS, H. The cellular network as a sensor: From mobile phone data to real-time road traffic monitoring. *IEEE Transactions on Intelligent Transportation Systems* 16, 5 (2015), 2551–2572.
- [20] JIN, M., HE, Y., FANG, D., CHEN, X., MENG, X., AND XING, T. iguard: A real-time anti-theft system for smartphones. *IEEE Transactions on Mobile Computing* (2018).
- [21] KAR, G., MUSTAFA, H., WANG, Y., CHEN, Y., XU, W., GRUTESER, M., AND VU, T. Detection of on-road vehicles emanating gps interference. In *Proceedings of the 2014 ACM SIGSAC Conference on Computer and Communications Security* (2014), ACM, pp. 621–632.
- [22] LANE, N. D., XU, Y., LU, H., HU, S., CHOUDHURY, T., CAMPBELL, A. T., AND ZHAO, F. Enabling large-scale human activity inference on smartphones using community similarity networks (csn). In *Proceedings of the 13th international conference on Ubiquitous computing* (2011), ACM, pp. 355–364.
- [23] LI, L., CHEN, L., HUANG, X., AND HUANG, J. A traffic congestion estimation approach from video using time-spatial imagery. In *Intelligent Networks and Intelligent Systems, 2008. ICINIS'08. First International Conference on* (2008), IEEE, pp. 465–469.
- [24] LIU, S., LIU, Y., NI, L., LI, M., AND FAN, J. Detecting crowdedness spot in city transportation. *IEEE Transactions on Vehicular Technology* 62, 4 (2013), 1527–1539.
- [25] MENG, C., CUI, Y., HE, Q., SU, L., AND GAO, J. Travel purpose inference with gps trajectories, pois, and geo-tagged social media data. In *Big Data (Big Data), 2017 IEEE International Conference on* (2017), IEEE, pp. 1319–1324.
- [26] MOHAMMADMORADI, H., GNAWALI, O., MOSS, D., BOELZLE, R., AND WANG, G. Effectiveness of a task-based residential energy efficiency program in oahu.
- [27] PAPAIOANNOU, S., MARKHAM, A., AND TRIGONI, N. Tracking people in highly dynamic industrial environments. *IEEE Transactions on Mobile Computing (Issue: 99)* (2016).
- [28] ROSE, G. Mobile phones as traffic probes: practices, prospects and issues. *Transport Reviews* 26, 3 (2006), 275–291.
- [29] SALEH, S. A. M., SUANDI, S. A., AND IBRAHIM, H. Recent survey on crowd density estimation and counting for visual surveillance. *Engineering Applications of Artificial Intelligence* 41 (2015), 103–114.
- [30] SHI, Q., AND ABDEL-ATY, M. Big data applications in real-time traffic operation and safety monitoring and improvement on urban expressways. *Transportation Research Part C: Emerging Technologies* 58 (2015), 380–394.
- [31] STATISTA. Number of internet users who used the internet for route planning, to access maps or road maps (e.g. google maps) in germany from 2013 to 2016, by frequency (in millions). <https://www.statista.com/statistics/432169/online-route-planning-and-map-usage-eg-google-maps-germany>, 2017.
- [32] TATEM, A. J. Worldpop, open data for spatial demography. *Scientific data* 4 (2017), 170004–170004.
- [33] THIAGARAJAN, A., RAVINDRANATH, L., BALAKRISHNAN, H., MADDEN, S., AND GIROD, L. Accurate, low-energy trajectory mapping for mobile devices.
- [34] THIAGARAJAN, A., RAVINDRANATH, L., LACURTS, K., MADDEN, S., BALAKRISHNAN, H., TOLEDO, S., AND ERIKSSON, J. Vtrack: accurate, energy-aware road traffic delay estimation using mobile phones. In *Proceedings of the 7th ACM conference on embedded networked sensor systems* (2009), ACM, pp. 85–98.
- [35] US DOT. Cv pilots take advantage of multiple communication media. https://www.its.dot.gov/pilots/cvp_media.htm, 2017.
- [36] WANG, D., ZHONG, W., YIN, Z., XIE, D., AND LUO, X. Spatio-temporal dynamics of population in shanghai: A case study based on cell phone

- signaling data. In *Big Data Support of Urban Planning and Management*. Springer, 2018, pp. 239–254.
- [37] WANG, H., CALABRESE, F., DI LORENZO, G., AND RATTI, C. Transportation mode inference from anonymized and aggregated mobile phone call detail records. In *Intelligent Transportation Systems (ITSC), 2010 13th International IEEE Conference on* (2010), IEEE, pp. 318–323.
- [38] WU, J., LI, K., JIANG, Y., LV, Q., SHANG, L., AND SUN, Y. Large-scale battery system development and user-specific driving behavior analysis for emerging electric-drive vehicles. *Energies* 4, 5 (2011), 758–779.
- [39] XIE, X., ZHANG, F., AND ZHANG, D. Privatehunt: Multi-source data-driven dispatching in for-hire vehicle systems. *Proceedings of the ACM on Interactive, Mobile, Wearable and Ubiquitous Technologies* 2, 1 (2018), 45.
- [40] YOON, J., NOBLE, B., AND LIU, M. Surface street traffic estimation. In *Proceedings of the 5th international conference on Mobile systems, applications and services* (2007), ACM, pp. 220–232.
- [41] ZANG, H., AND BOLOT, J. Anonymization of location data does not work: A large-scale measurement study. In *Proceedings of the 17th annual international conference on Mobile computing and networking* (2011), ACM, pp. 145–156.
- [42] ZHANG, D., ZHAO, J., ZHANG, F., AND HE, T. Urbancps: a cyber-physical system based on multi-source big infrastructure data for heterogeneous model integration. In *Proceedings of the ACM/IEEE Sixth International Conference on Cyber-Physical Systems* (2015), ACM, pp. 238–247.
- [43] ZHANG, T., LENG, N., AND BANERJEE, S. A vehicle-based measurement framework for enhancing whitespace spectrum databases. In *Proceedings of the 20th annual international conference on Mobile computing and networking* (2014), ACM, pp. 17–28.
- [44] ZHAO, Y., LI, S., HU, S., SU, L., YAO, S., SHAO, H., WANG, H., AND ABDELZAHHER, T. Greendrive: A smartphone-based intelligent speed adaptation system with real-time traffic signal prediction. In *Cyber-Physical Systems (ICCPs), 2017 ACM/IEEE 8th International Conference on* (2017), IEEE, pp. 229–238.
- [45] ZHENG, Z., WANG, D., PEI, J., YUAN, Y., FAN, C., AND XIAO, F. Urban traffic prediction through the second use of inexpensive big data from buildings. In *Proceedings of the 25th ACM International on Conference on Information and Knowledge Management* (2016), ACM, pp. 1363–1372.
- [46] ZHOU, P., ZHENG, Y., AND LI, M. How long to wait?: predicting bus arrival time with mobile phone based participatory sensing. In *Proceedings of the 10th international conference on Mobile systems, applications, and services* (2012), ACM, pp. 379–392.
- [47] ZHOU, P., ZHENG, Y., AND LI, M. How long to wait? predicting bus arrival time with mobile phone based participatory sensing. *IEEE Transactions on Mobile Computing* 13, 6 (2014), 1228–1241.
- [48] ZHU, Y., CHEN, C., AND GAO, M. An evaluation of vehicular networks with real vehicular gps traces. *EURASIP Journal on Wireless Communications and Networking* 2013, 1 (2013), 190.